ISSN 1674-1056
http://cpb.iphy.ac.cn
http://iopscience.iop.org/cpb
中国物理 B
Chinese Physics
中国物理 Chinese Physics B

Improved electrochemical performances of $Li(Ni_{0.6}Co_{0.2}Mn_{0.2})O_2$ at high charging cut-off voltage with $Li_{1.4}Al_{0.4}Ti_{1.6}(PO_4)_3$ surface coating

Yi Wang(王怡), Bo-Nan Liu(刘柏男), Ge Zhou(周格), Kai-Hui Nie(聂凯会), Jie-Nan Zhang(张杰男), Xi-Qian Yu(禹习谦), Hong Li(李泓)

Citation: Chin. Phys. B . 2019, 28(6): 068202. **doi:** 10.1088/1674-1056/28/6/068202
Journal homepage: http://cpb.iphy.ac.cn; http://iopscience.iop.org/cpb

What follows is a list of articles you may be interested in

Improved electrochemical performances of high voltage $LiCoO_2$ with tungsten doping

Jie-Nan Zhang(张杰男), Qing-Hao Li(李庆浩), Quan Li(李泉), Xi-Qian Yu(禹习谦), Hong Li(李泓)
Chin. Phys. B . 2018, 27(8): 088202. **doi:** 10.1088/1674-1056/27/8/088202

First principle study of $LiXS_2$ (X = Ga, In) as cathode materials for Li ion batteries

Feng-Ya Rao(饶凤雅), Fang-Hua Ning(宁芳华), Li-Wei Jiang(蒋礼威), Xiang-Ming Zeng(曾祥明), Mu-Sheng Wu(吴木生), Bo Xu(徐波), Chu-Ying Ouyang(欧阳楚英)
Chin. Phys. B . 2016, 25(2): 028202. **doi:** 10.1088/1674-1056/25/2/028202

Lithium-ion transport in inorganic solid state electrolyte

Jian Gao(高健), Yu-Sheng Zhao(赵予生), Si-Qi Shi(施思齐), Hong Li(李泓)
Chin. Phys. B . 2016, 25(1): 018211. **doi:** 10.1088/1674-1056/25/1/018211

Surface structure evolution of cathode materials for Li-ion batteries

Yingchun Lyu(吕迎春), Yali Liu(刘亚利), Lin Gu(谷林)
Chin. Phys. B . 2016, 25(1): 018209. **doi:** 10.1088/1674-1056/25/1/018209

Strategies to curb structural changes of lithium/transition metal oxide cathode materials & the changes' effects on thermal & cycling stability

Xiqian Yu(禹习谦), Enyuan Hu(胡恩源), Seongmin Bak,Yong-Ning Zhou(周永宁), Xiao-Qing Yang(杨晓青)
Chin. Phys. B . 2016, 25(1): 018205. **doi:** 10.1088/1674-1056/25/1/018205

Improved electrochemical performance of $Li(Ni_{0.6}Co_{0.2}Mn_{0.2})O_2$ at high charging cut-off voltage with $Li_{1.4}Al_{0.4}Ti_{1.6}(PO_4)_3$ surface coating*

Yi Wang(王怡)[1,2], Bo-Nan Liu(刘柏男)[3], Ge Zhou(周格)[1,2], Kai-Hui Nie(聂凯会)[1,2], Jie-Nan Zhang(张杰男)[1,‡], Xi-Qian Yu(禹习谦)[1,2,†], and Hong Li(李泓)[1,2,3]

[1] *Key Laboratory for Renewable Energy, Beijing Key Laboratory for New Energy Materials and Devices, Beijing National Laboratory for Condensed Matter Physics, Institute of Physics, Chinese Academy of Sciences, Beijing* 100190, *China*
[2] *School of Physical Sciences, University of Chinese Academy of Sciences, Beijing* 100190, *China*
[3] *IOPSILION Co., Ltd., Liyang* 213300, *China*

(Received 19 February 2019; revised manuscript received 18 March 2019; published online 8 May 2019)

$Li(Ni_{0.6}Co_{0.2}Mn_{0.2})O_2$ has been surface-modified by the lithium-ion conductor $Li_{1.4}Al_{0.4}Ti_{1.6}(PO_4)_3$ via a facile mechanical fusion method. The annealing temperature during coating process shows a strong impact on the surface morphology and chemical composition of $Li(Ni_{0.6}Co_{0.2}Mn_{0.2})O_2$. The 600-°C annealed material exhibits the best cyclic stability at high charging cut-off voltage of 4.5 V (*versus* Li^+/Li) with the capacity retention of 90.9% after 100 cycles, which is much higher than that of bare material (79%). Moreover, the rate capability and thermal stability are also improved by $Li_{1.4}Al_{0.4}Ti_{1.6}(PO_4)_3$ coating. The enhanced performance can be attributed to the improved stability of interface between $Li(Ni_{0.6}Co_{0.2}Mn_{0.2})O_2$ and electrolyte by $Li_{1.4}Al_{0.4}Ti_{1.6}(PO_4)_3$ modification. The results of this work provide a possible method to design reliable cathode materials to achieve high energy density and long cycle life.

Keywords: lithium-ion batteries, cathode, Ni-rich oxide, solid electrolyte, coating

PACS: 82.47.Aa, 82.45.Fk **DOI:** 10.1088/1674-1056/28/6/068202

1. Introduction

Lithium-ion batteries (LIBs) have become the most suitable candidates for use in modern society because of their high energy density, long cycle life, and environmentally friendly characteristics. Further increasing the energy density and reducing the cost have become important directions for the development of LIBs.[1] $Li(Ni_xCo_yMn_z)O_2$ (denoted as NCM, $x+y+z=1$) has attracted wide research attention as a high density cathode material due to its higher discharge capacities and lower cost than cobalt based cathode materials.[2]

The attainable capacity of NCM at the same charging cut-off voltage increases with the increase of Ni content. However, the higher Ni content leads to more significant irreversible structural transformation in the course of lithium extraction, posing great challenges for the development of NCM oxides with higher Ni content. At present, $Li(Ni_{0.6}Co_{0.2}Mn_{0.2})O_2$ (NCM622) is one of the NCM cathode materials close to commercialization with good cyclic stability and acceptable level of safety performance. The practical reversible capacity of NCM622 is about 170 mAh/g at a charging voltage of 4.3 V (*versus* Li^+/Li), which is much lower than the theoretic capacity (277 mAh/g).[3,4] If a higher charging voltage can be reached, then the usable capacity will be further improved. However, NCM622 suffers from poor cycle stability and severe safety issues especially at higher charging voltage. Unstable surface and interface characteristics are the main causes of these problems. The irreversible phase transitions from layered structure to spinel and NiO-type rock-salt phases at particles surface accompanied by the transition metal dissolution will cause a series of problems such as the capacity decay and gas release.[5,6] Furthermore, the unstable interface between the electrode and electrolyte is another main challenge to the successful application of NCM622 at high voltage. The decomposition of electrolyte and formation of cathode electrode interphase (CEI) may increase the interfacial resistance, and block the transportation of Li-ion and exhaust electrolyte.[7,8] Numerous studies have been devoted to improving the cyclic stability of NCM622 using various kinds of approaches. Detailed technical strategies include surface coating, concentration gradient design, and adding additives into the electrolyte.[9,10]

Surface coating has been considered as the most effective approach to protect the particles of NCM622. Of the various coating materials, oxides are the most commonly used ones. By coating with Al_2O_3, TiO_2, ZrO_2, *etc*., the cyclic stability of NCM622 materials can be greatly improved.[11–13] However, these oxide coating materials are often electronic insulators with poor Li-ion conductivity, which will introduce ad-

*Project supported by the National Key Research and Development Program of China (Grant No. 2017YFB0102004), the National Natural Science Foundation of China (Grant No. 51822211), and the State Grid Technology Project, China (Grant No. DG71-17-010).

†Corresponding author. E-mail: jnzhang@iphy.ac.cn
‡Corresponding author. E-mail: xyu@iphy.ac.cn

© 2019 Chinese Physical Society and IOP Publishing Ltd

ditional resistance to Li-ion diffusion and charge transfer at surface. To solve this problem, Li-ion conductors are likely to be more promising coating materials. Solid electrolytes such as Li_3PO_4, $Li_{1.4}Al_{0.4}Ti_{1.6}(PO_4)_3$ (LATP), and $Li_7La_3Zr_2O_{12}$ (LLZO) are good choices because of high Li-ion conductivity and wide electrochemical window.[14–16] Among them, Na super ionic conductor (NASICON)-type LATP shows great potential for practical application for its low cost and preferable performance. In previous studies, LATP has been successfully coated on $Li_{1.2}Ni_{0.13}Co_{0.13}Mn_{0.54}O_2$ and $LiCoO_2$, and the coated materials showed good cyclic stability due to the stable interface between cathode materials and electrolyte.[17,18] Choi *et al.* first introduced LATP into the NCM622 as a coating material and proved it an effective method to improve the cell performance (charging cut-off voltage of 4.3 V).[19] However, the coating effects of LATP at higher charging cut-off voltage have not been systematically studied.

In this work, LATP modified NCM622 oxides have been synthesized using a simple mechanical fusion method. The influences of heat-treatment temperatures on the electrochemical performance of LATP coated NCM622 samples are systematically studied. The 600-°C heat-treated sample shows significantly improved electrochemical performance with the best cycle performance at a high charging cut-off voltage of 4.5 V.

2. Experiment

2.1. Synthesis

The $LiNi_{0.6}Co_{0.2}Mn_{0.2}O_2$ was prepared by solid-state sintering method. The mixture of the commercial precursor $[Ni_{0.6}Co_{0.2}Mn_{0.2}](OH)_2$ and $LiOH{\cdot}H_2O$ powders was first heated at 450 °C for 5 h and then heated at 850 °C for 15 h in air to obtain the $LiNi_{0.6}Co_{0.2}Mn_{0.2}O_2$ powder. For the synthesis of LATP, Li_2CO_3, Al_2O_3, TiO_2, and $NH_2H_2PO_4$ precursors were ground by ball milling and heated at 400 °C for 2 h followed by 900 °C for 5 h in air. Then, the obtained LATP was ground through a pulverizer to reduce the particle size down to hundreds of nanometers. Finally, 1-wt% LATP was introduced to the NCM622 powder by 20 minutes mechanical fusion with a mechanical fusion machine (VSH, China). The obtained materials were heated in air for 4 h at 400 °C, 500 °C, 600 °C, and 700 °C, respectively, to get the final LATP modified NCM622 materials (denoted as LATP-NCM-400, LATP-NCM-500, LATP-NCM-600, and LATP-NCM-700).

2.2. Characterization

The morphology of bare and LATP modified NCM622 materials were characterized by a field emission scanning electron microscope (FE-SEM, S4800, Hitachi) with energy dispersive spectrometer (EDS). The x-ray diffraction (XRD) data were obtained in the scan range (2θ) of 10°–85° with an increment of 0.02° on an x-ray diffractometer of D8 Advance, Bruker (Cu Kα radiation). The electronic conductivity was conducted by the powder impedance instrument (Mitsubishi MCP-PD51) using four probe method. The 3-g powder was placed into a 2-cm diameter cylinder mold. Then, the electronic conductivity was tested under different pressures from 6 kN to 18 kN. The x-ray photoelectron spectroscopy (XPS) was recorded by an ESCALAB 250 Xi, Thermo Fisher with monochromatic 150-W Al Kα radiation. XPS data were analyzed by Avantage and the binding energies were calibrated by the C 1s line at 284.8 eV. The differential scanning calorimetry/thermal gravimetric (DSC/TG) measurements were performed on simultaneous thermal analyzer (Netzsch STA 449C). For this analysis, cells were charged to 4.5 V at 0.1 C (1 C = 190 mA/g), and then disassembled in an argon filled glovebox to get the charged electrodes. The delithiated electrode was heated in an Al_2O_3 crucible under argon with a heating rate of 10 °C/min.

2.3. Electrochemical measurement

The working electrodes were prepared by casting the mixture of cathode material 80.0 wt%, super P 10.0 wt%, and polytetrafluoroethylene (PVDF) 10.0-wt% dissolved with N-methyl pyrrolidone (NMP) solvent onto Al foil (12 μm in thickness). The electrodes were punched into disks and then dried at 120 °C in vacuum for 12 hours. The loading mass of active material in the electrode is around 3 mg/cm^2. The electrochemical performance was tested using CR 2032 coin cell, assembled in a glove box filled with argon. 1-M $LiPF_6$ in ethylene carbonate (EC) and dimethyl carbonate (DMC) (1:1 in volume) was used as electrolyte. Li foil (500 μm) was used as the counter electrode and Al_2O_3 coated polyethylene (15 μm) was used as the separator. The charge and discharge tests were carried out using a Land CT2001A battery test system (Land, Wuhan, China) at room temperature. The electrochemical impedance spectroscopy (EIS) measurements were performed at 25 °C by using an IM6e impedance analyzer with a perturbation of 5 mV in the frequency range 25 mHz–1 MHz.

3. Results and discussion

The morphology of bare NCM622, LATP, and LATP modified samples are shown in Fig. 1. The surface of bare NCM622 is smooth and clean, and the secondary microspheres consist of primary particles with a size of 300 nm–700 nm (Figs. 1(a) and 1(b)). The inset of Fig. 1(a) shows the morphology of LATP, whose diameter is in the range of 200 nm–500 nm. The detailed morphology of the LATP modified NCM622 with different annealing temperatures of 400 °C, 500 °C, 600 °C, and 700 °C is displayed in Figs. 1(c)–1(f), respectively. It can be seen that the LATP nano sheets are uniformly distributed on the surface of LATP-NCM-400. As the annealing temperature increases to above 600 °C, the LATP

nano-particles begin to disappear gradually and the coated LATP layer becomes almost invisible at 700 °C. This phenomenon indicates the "melting" of the LATP coating layer and likely the diffusion into the interior of the NCM622 particle. To further confirm that the LATP still exists on the surface of the cathode particles, EDS mapping is performed to investigate the elemental distribution on the surface of LATP-NCM-700 (Fig. 2). It is clear that the Ti, Al, and P elements are uniformly distributed on the surface of NCM622, indicating the homogeneous distribution of LATP.

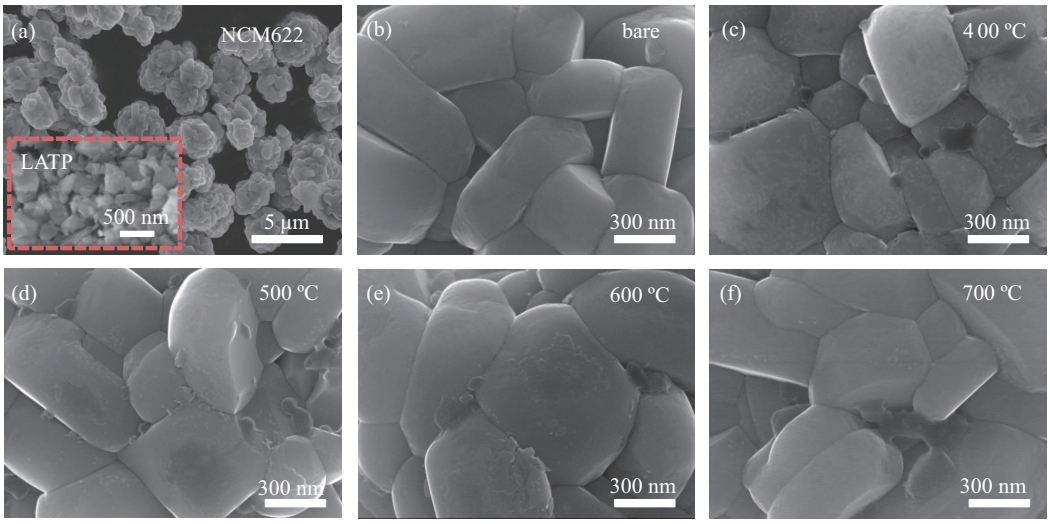


Fig. 1. SEM images of (a) bare NCM622 at low magnification with raw LATP in the inset, (b) bare NCM 622 at high magnification, and 1-wt% LATP modified NCM622 after annealing at (c) 400 °C, (d) 500 °C, (e) 600 °C, and (f) 700 °C.

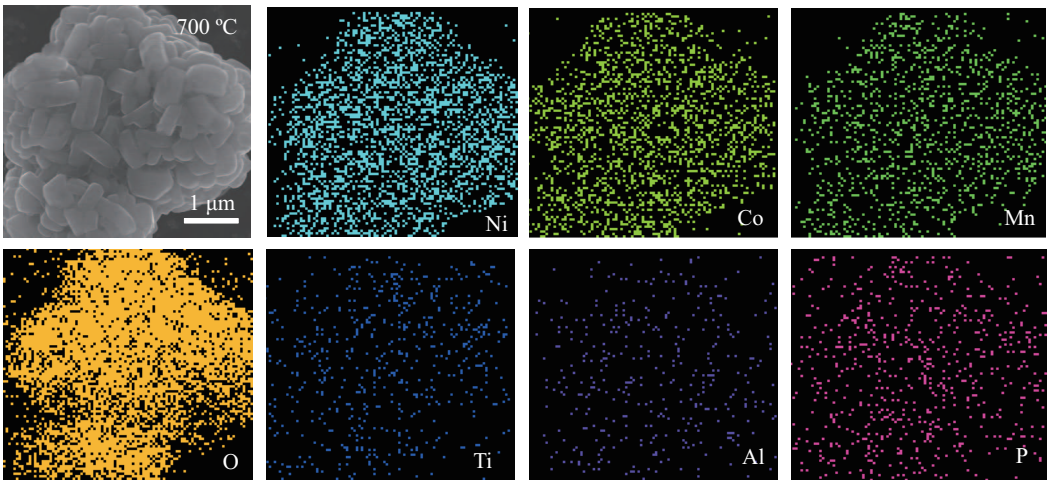


Fig. 2. EDS mappings of LATP-NCM-700 particle.

To understand the influence of LATP coating process on the bulk structure of NCM622, XRD measurements are conducted and the results are shown in Fig. 3. All main peaks can be indexed to the hexagonal α-$NaFeO_2$ structure with space group of R-3m without an indication of secondary phase. All XRD patterns show the splitting of (006)/(012) and (018)/(110) peaks, which verifies a well-grown layered structure.[20] In addition, it is generally accepted that the peak intensity ratio of $I_{(003)}/I_{(104)}$ is related to the degree of cation mixing.[21] The value is 1.43 for bare NCM622 and increases to more than 1.68 for these LATP modified NCM622 samples, indicating a less extent of cation mixing after heat treatment. These experimental results suggest that the LATP modification does not obviously change the crystal structure or introduce an impurity phase of NCM622.

The influence of LATP on the electronic conductivity of NCM622 is also investigated by powder impedance measurements. As shown in Fig. 4, the electronic conductivity of LATP modified samples is lower than the bare one due to the electronic insulation characteristic of LATP. The electronic conductivity decreases gradually from 400 °C to 600 °C, which is correlated with the growing up process of LATP nano-particles during heating process. While at 700 °C, the LATP particles have totally diffused into NCM622 surface, leading to the recovery of electronic conductivity. These results are consistent with the SEM images.

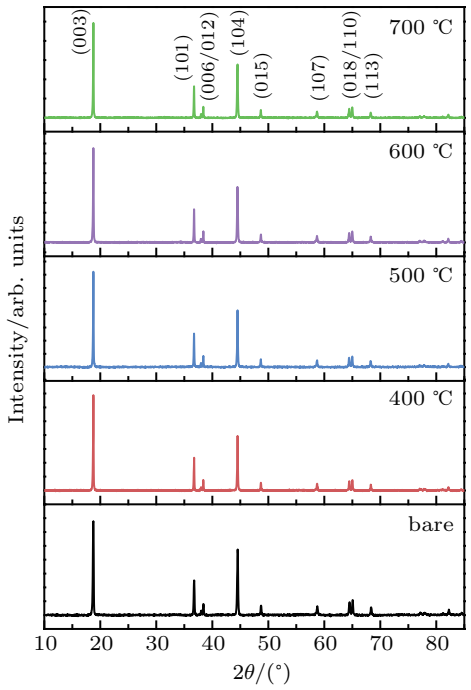


Fig. 3. XRD patterns of bare and LATP modified NCM622 materials.

To further study the surface chemical status of the bare NCM622 and LATP modified NCM622, XPS measurements are performed. Figure 5 shows the O 1s, P 2p, Ti 2p, and Ni 2p XPS spectra for different samples. The first narrow peak at 529.1 eV in all O 1s spectra (Fig. 5(a)) is related to the lattice oxygen in NCM622, while the second peak at 531.6 eV can be entirely attributed to the Li_2CO_3 residual. Li_2CO_3 often appears on layered oxide cathode materials resulting from the chemical reaction with H_2O and CO_2 in the air, especially for the Ni-rich materials.[22] This peak shifts to 531.3 eV for LATP modified NCM622 due to the P–O bond in LATP. However, it is rather difficult to clearly separate the signal from CO_3^{2-} and P–O bond in this broad peak. The P 2p spectra shown in Fig. 5(b) further prove the existence of P–O bond. The peak positions of P-O bond in both O 1s and P 2p spectra are almost unchanged for different heat treated samples, indicating the similar chemical environment between P and O ions. The Ti 2p peaks gradually shift to low binding energy side as the temperature increases (Fig. 5(c)), which is likely due to the chemical reaction between LATP and NCM622. At the same time, there is no oxidation state change of Ni, as shown in Fig. 5(d), demonstrating that the coating process does not affect the surface composition of NCM622 obviously.

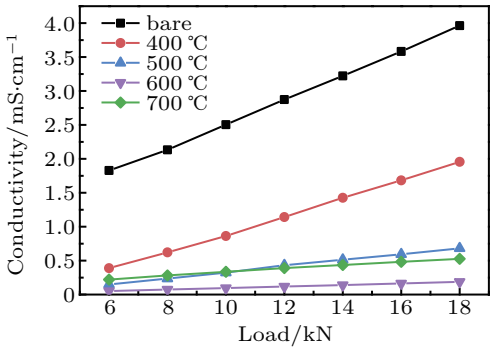


Fig. 4. The electronic conductivity of bare and LATP modified NCM622 materials.

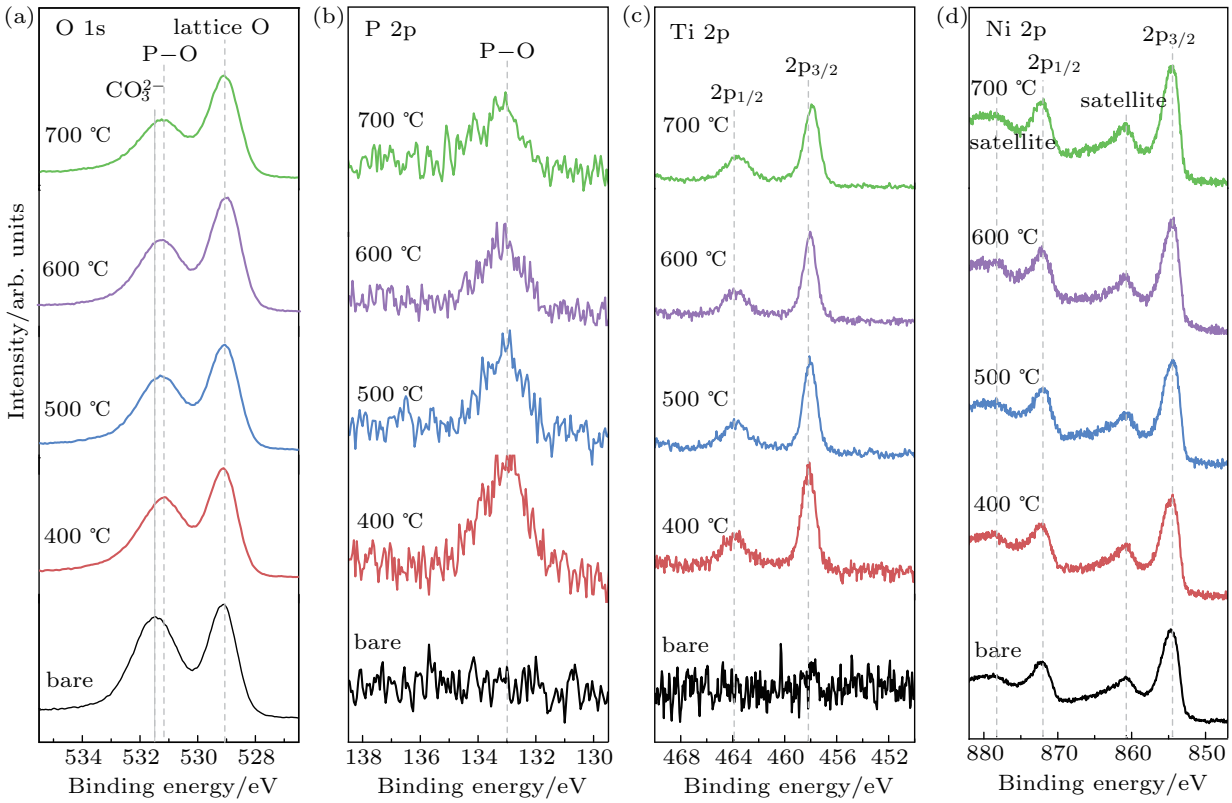


Fig. 5. The O 1s (a), P 2p (b), Ti 2p (c), and Ni 2p (d) XPS spectra of bare and LATP modified NCM622 materials.

Quantitative analysis of O 1s and P 2p XPS spectra is conducted to reveal the change of surface composition for different NCM622 samples. Due to the overlap of the peaks of CO_3^{2-} and P–O in O 1s spectra, accurate determination of the quantity for CO_3^{2-} and P–O only by O 1s spectra is very difficult. Considering PO_4^{3-} (P:O = 1:4) in LATP, the content of P–O peak in O 1s is estimated by four times the content of P-O in P 2p. As shown in Fig. 6(a), the relative ratio of XPS signal from lattice oxygen increases with temperature, indicating that the exposure of more NCM622 particle surface after high temperature annealing process. Meanwhile, the amount of Li_2CO_3 on LATP modified NCM622 samples is obviously reduced compared to the bare NCM622. And it decreases slightly with the increase of the annealing temperature. According to the previous literature, the Li_2CO_3 induced by side reactions with air or moisture exposure could cause poor electrochemical performance of layered oxide cathode at high charging cut-off voltage.[23,24] Moreover, the content of P–O reduces with the increase of temperature, indicating the diffusion of LATP into the NCM622 surface at high temperature. This is consistent with the SEM observations. Based on these results, the change of NCM622 surface after LATP modification during heat treatment is concluded by the schematic diagram, as shown in Fig. 6(b).

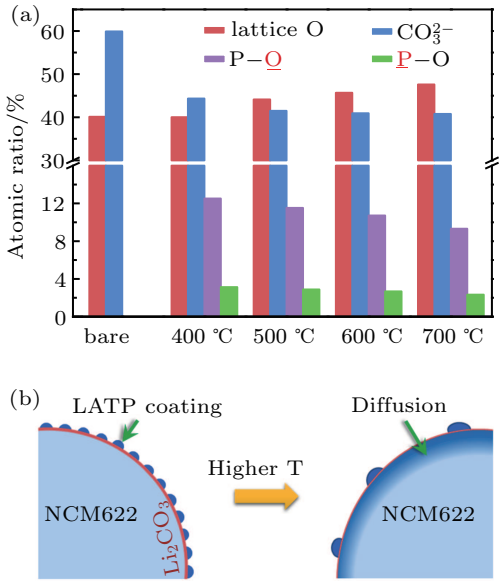


Fig. 6. (a) Quantitative analysis of O 1s and P 2p XPS spectra of bare and LATP modified NCM622 materials. (b) Schematic diagram for the surface evolution of LATP modified NCM622 during annealing process.

The electrochemical performance of bare and LATP modified NCM622 are evaluated to verify the effect of coating. Figure 7(a) exhibits the initial charge/discharge curves at 1 C (1 C = 190 mA/g) between 2.8 V and 4.5 V for bare and LATP modified NCM622 samples. The initial discharge capacities for different samples are summarized in Table 1. Except for LATP-NCM-600, the modified materials show slightly lower discharge capacities than the bare one. The cycling stability of different samples at 1 C in the voltage range of 2.8 V–4.3 V and 2.8 V–4.5 V is shown in Figs. 7(b) and 7(c), respectively. The values of the initial and 100th-cycle discharge capacities and the capacity retention ratios are summarized in Table 1. For the bare NCM622 materials cycled at 4.3 V, relatively stable cycle performance can be achieved with 91.7% of capacity retention after 100 cycles. The capacity retention ratios increase for these LATP modified NCM622 samples. Among them, LATP-NCM-600 exhibits the highest capacity retention of 98.2% over 100 cycles followed by LATP-NCM-700, LATP-NCM-500, and LATP-NCM-400. The initial capacity can be further improved about 20 mAh/g by increasing the charging cut-off voltage to 4.5 V, but this benefit is always counteracted by the degraded electrochemical stability. For the bare NCM622, the capacity retention value drops from 91.7% to 79% after 100 cycles. However, much better capacity retention can be achieved for LATP-NCM-600 (98.2%, 4.3 V *versus* 90.9%, 4.5 V), indicating that LATP modification can greatly improve the performance of NCM622, even at high voltage. The extent of the improvement is affected by the

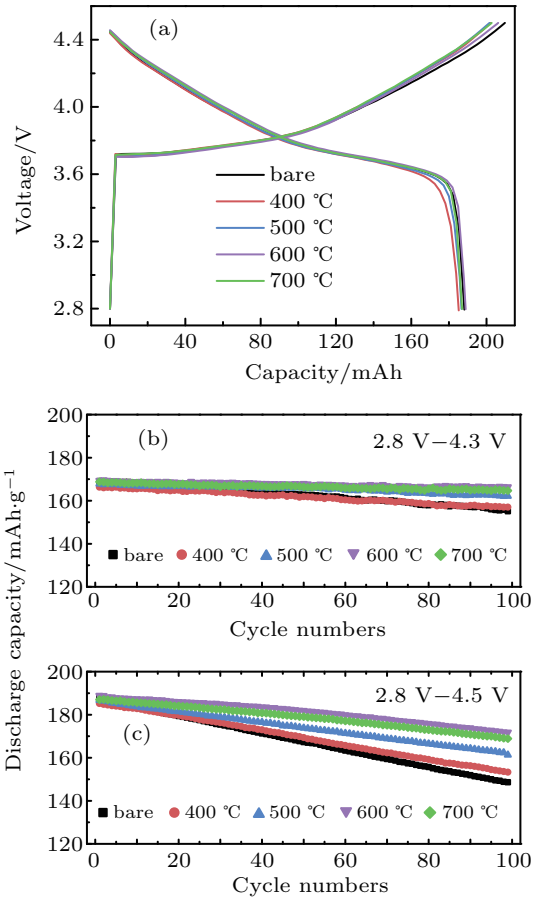


Fig. 7. (a) The initial charge and discharge curves for bare and LATP modified NCM622 cathodes cycled in the voltage range of 2.8 V–4.5 V. Cycle performance in the voltage range of (b) 2.8 V–4.3 V and (c) 2.8–4.5 V for bare and LATP modified NCM622 cathodes. All cells were cycled at 1 C rate (1 C = 190 mA/g).

annealing temperature during the coating process. The detailed mechanism can be attributed to different surface conditions of LATP modified NCM622 under various temperatures. It can be proposed that the suitable content of surface doping and coating of LATP can be achieved on LATP-NCM-600 according to the SEM and XPS results. This surface modified layer can effectively reduce the side reaction by avoiding the direct contact between cathode materials and electrolyte, and inhibit the harmful phase transition on the surface of NCMM622 by doping of P, Ti, and Al ions.

Table 1. Typical discharge capacity values of various NCM622 (unit: mAh/g).

	Cycle number	Bare NCM622	400 °C	500 °C	600 °C	700 °C
2.8 V–4.3 V	1st	169.1	166.3	167.8	169.4	168.6
	100th	155.1	157.0	162.2	166.4	164.7
Capacity retention ratio		91.7%	94.4%	96.7%	98.2%	97.7%
2.8 V–4.5 V	1st	188.2	185.2	186.7	188.9	187.1
	100th	148.6	153.7	161.3	171.8	168.9
Capacity retention ratio		79.0%	83.0%	86.4%	90.9%	90.3%

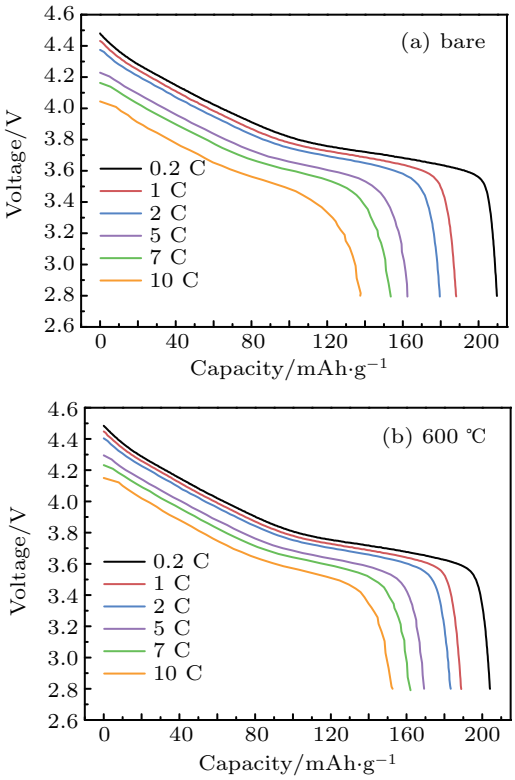


Fig. 8. Discharge curves of (a) bare NCM622 and (b) LATP-NCM-600 at different current densities between 2.8 V and 4.5 V.

The rate performance of bare NCM622 and LATP-NCM-600 in the voltage range of 2.8 V–4.5 V are further studied, as shown in Fig. 8. The fact that the capacity at 0.2 C for LATP-NCM-600 is lower than the bare one may result from the decreased electronic conductivity (Fig. 4). While at a current rate above 1 C, LATP-NCM-600 exhibits superior rate capability. Even at a high discharging rate of 10 C (1 C = 190 mA/g), LATP-NCM-600 still maintains a discharge capacity as high as 152.6 mAh/g, which is much higher than the bare one (137.5 mAh/g). In addition, the discharge voltage fading for bare NCM622 is more severe at high current density than LATP-NCM-600. The reduced polarization and improved capacity retention of LATP-NCM-600 can be attributed to the optimized surface properties and the high Li^+ conductivity of LATP.

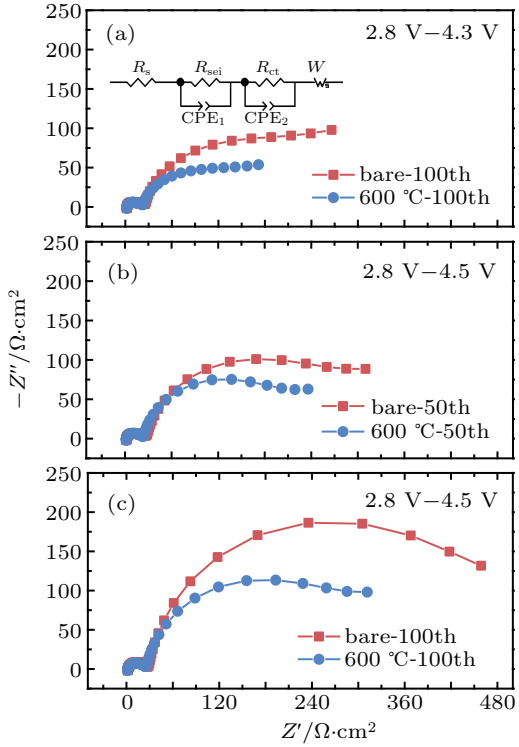


Fig. 9. The EIS curves of bare NCM622 and LATP-NCM-600/Li half cells measured after (a) the 100th cycle in the range of 2.8 V–4.3 V with an inset image of the equivalent circuit model, (b) the 50th, and (c) 100th cycle in the range of 2.8 V–4.5 V. The spectra were collected at 25 °C between 1 MHz and 25 mHz with a voltage amplitude of 5 mV.

EIS measurements are performed to understand the reasons for the improvement of electrochemical performance. The EIS spectra for half cells with bare NCM622 and LATP-NCM-600 sample are measured after the 100th cycle with a cutoff voltage of 4.3 V and after the 50th and 100th cycles with a cutoff voltage of 4.5 V, as shown in Figs. 9(a), 9(b), and 9(c), respectively. Three regions can be recognized in these spectra, including a high frequency semicircle ascribed to cathode/solid electrolyte interphase (CEI/SEI) formation (R_{SEI}), a

mediate frequency semicircle ascribed to charge transfer process (R_{ct}), and a short slope line at low frequency ascribed to diffusion process (W). The equivalent circuit is given in the inset of Fig. 9(a). Note that the slope line is completely absent for bare NCM in Fig. 9(c) due to the slow charge transfer process after 100 cycles. After cycling, the R_{SEI} for LATP-NCM-600 is slightly lower than the bare material, while the R_{ct} changes a lot by LATP modification, especially at high voltage and after repeated cycling. It can be proposed that the dramatic increasing of R_{ct} for bare NCM622 during cycling leads to the rapid performance decay. With the LATP modification, the surface side reaction and irreversible phase transition could be partial inhibited, leading to a stable interface independence of LATP-NCM-600.

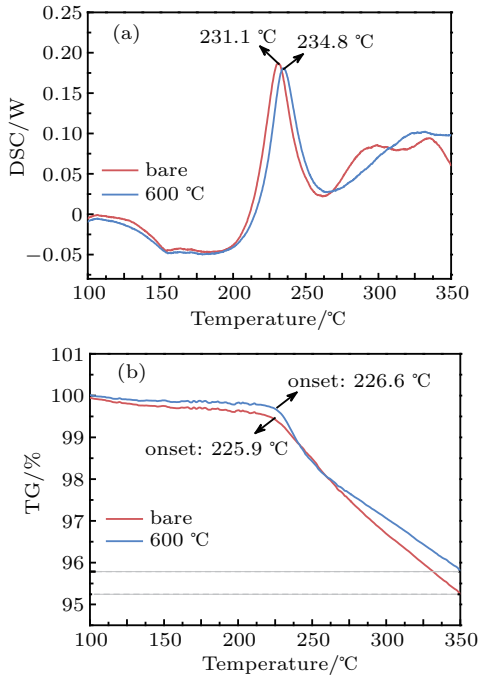


Fig. 10. (a) The DSC and (b) TG curves for bare NCM622 and LATP-NCM-600 electrodes after the first charge to 4.5 V.

In addition to the electrochemical performance, thermal stability is another major concern for the large-scale application of cathode materials. Layered oxide cathodes with high nickel content at high delithiated state often show accelerated thermal runaway due to the rapid Ni reduction and oxygen release.[25] Surface modification has been reported as an effective method to enhance thermal stability. DSC/TG measurements are carried out to compare the thermal stability between bare NCM622 and LATP-NCM-600. After charging to 4.5 V, the exothermic reaction of bare NCM622 is initiated at 231.1 °C (Fig. 10(a)), which can be attributed to the transition metal reduction and O_2 release of NCM622. After LATP modification, the initial temperature of this exothermic peak delays to appear at higher temperature (234.8 °C). The TG results in Fig. 10(b) also exhibit a deferred starting temperature of weight loss and mitigated weight loss amount for LATP-NCM-600 compared to the bare one. These results illustrate the improved thermal stability of NCM622 by LATP coating.

4. Conclusion

In conclusion, solid electrolyte LATP has been employed as a coating material for NCM622 cathode through a simple mechanical fusion method, which shows that the electrochemical performance and thermal stability of NCM622 have been greatly improved after coating. Among these LATP modified samples, 600-°C annealed material exhibits the best cyclic stability even at a high charging cut-off voltage of 4.5 V. The enhanced performance can be attributed to the improved interfacial properties by LATP modification, which reduces surface Li_2CO_3 impurity and enhances the stability and charge transfer process on surface. This work highlights that the solid electrolytes may be promising candidates as coating materials for the next generation high energy density cathode materials and the treating temperature is very important for the coating process.

References

[1] Goodenough J B and Kim Y 2010 *Chem. Mater.* **22** 587
[2] Kim J, Lee H, Cha H, Yoon M, Park M and Cho J 2018 *Adv. Energy Mater.* **8** 1702028
[3] Zhang Y, Cao H, Zhang J and Xia B 2006 *Solid State Ionics* **177** 3303
[4] Jo C H, Cho D H, Noh H J, Yashiro H, Sun Y K and Myung S T 2015 *Nano Res.* **8** 1464
[5] Cho Y, Oh P and Cho J 2013 *Nano Lett.* **13** 1145
[6] Jung S K, Gwon H, Hong J, Park K Y, Seo D H, Kim H, Hyun J, Yang W and Kang K 2014 *Adv. Energy Mater.* **4** 1300787
[7] Haik O, Leifer N, Samuk-Fromovich Z, Zinigrad E, Markovsky B, Larush L, Goffer Y, Goobes G and Aurbach D 2010 *J. Electrochem. Soc.* **157** A1099
[8] Zhang J N, Li Q, Wang Y, Zheng J, Yu X and Li H 2018 *Energy Storage Mater.* **14** 1
[9] Liu W, Oh P, Liu X, Lee M J, Cho W, Chae S, Kim Y and Cho J 2015 *Angew. Chem. Int. Ed.* **54** 4440
[10] Liao B, Hu X, Xu M, Li H, Yu L, Fan W, Xing L, Liao Y and Li W 2018 *J. Phys. Chem. Lett.* **9** 3434
[11] Chen Y, Zhang Y, Chen B, Wang Z and Lu C 2014 *J. Power Sources* **256** 20
[12] Tao T, Chen C, Yao Y, Liang B, Lu S and Chen Y 2017 *Ceram. Int.* **43** 15173
[13] Xiong D, Hynes T, Ellis L and Dahn J 2017 *J. Electrochem. Soc.* **164** A3174
[14] Lee S W, Kim M S, Jeong J H, Kim D H, Chung K Y, Roh K C and Kim K B 2017 *J. Power Sources* **360** 206
[15] Ling S G, Peng J Y, Yang Q, Qiu J L, Lu J Z and Li H 2018 *Chin. Phys. B* **27** 038201
[16] Gao J, Zhao Y S, Shi S Q and Li H 2016 *Chin. Phys. B* **25** 018211
[17] Yang Q, Huang J, Li Y, Wang Y, Qiu J, Zhang J, Yu H, Yu X, Li H and Chen L 2018 *J. Power Sources* **388** 65
[18] Wang T, Yang Z, Jiang Y, Li G and Huang Y 2016 *RSC Adv.* **6** 63749
[19] Choi J W and Lee J W 2016 *J. Power Sources* **307** 63
[20] Liu H, Qian D, Verde M G, Zhang M, Baggetto L, An K, Chen Y, Carroll K J, Lau D, Chi M, Veith G M and Meng Y S 2015 *ACS Appl. Mater. Interfaces* **7** 19189
[21] Li D, Sasaki Y, Kobayakawa K and Sato Y 2006 *J. Power Sources* **157** 488
[22] Lyu Y, Liu Y and Gu L 2016 *Chin. Phys. B* **25** 018209
[23] Chen Z and Dahn J R 2004 *Electrochim. Acta* **49** 1079
[24] Zhang J N, Li Q H, Li Q, Yu X Q and Li H 2018 *Chin. Phys. B* **27** 088202
[25] Yu X, Hu E, Bak S, Zhou Y N and Yang X Q 2016 *Chin. Phys. B* **25** 018205